Desalination and Water Treatment
www.deswater.com
doi: 10.5004/dwt.2023.30004

311 (2023) 85–91
November

Impregnating multi-walled carbon nanotubes with Cyanex 923 extractant to improve harmful chromium(VI) adsorption from aqueous media

Francisco Jose Alguacil*, Jose Ignacio Robla

Centro Nacional de Investigaciones Metalurgicas (CSIC), Avda. Gregorio del Amo 8, 28040 Madrid, Spain, email: fjalgua@cenim.csic.es (), jrobla@cenim.csic.es (J.I. Robla)

Received 5 June 2023; Accepted 26 September 2023

ABSTRACT

The performance of C923-impregnated multi-walled carbon nanotubes on harmful Cr(VI) adsorption from acidic solutions was investigated. C923 (Cyanex 923) is a liquid–liquid extraction reagent of the phosphine oxide type. The adsorption was investigated at various experimental conditions: stirring speed (250–1,500 min^{-1}, temperature (20°C–60°C), HCl (0.5–2 M) and metal (0.01–0.2 g/L) concentrations in the aqueous phase, ionic strength of this phase, and adsorbent dosage (0.5–1 g/L). It was found that the metal adsorption is endothermic and spontaneous, responded to the moving boundary rate law and to the Freundlich isotherm. Adsorption dosage responded to two different models, at 0.5 g/L, data were fitted to the first order kinetic equation, whereas at 1 g/L, pseudo-second-order model fitted to the experimental results. Metal loaded onto the impregnated nanotubes can be desorbed by the use of hydrazine sulphate solutions, at the same time, chromium was recovered in the solutions in the less harmful Cr(III) oxidation state.

Keywords: Chromium(VI); Multi-walled carbon nanotubes; Cyanex 923; Adsorption; Desorption

1. Introduction

Chromium(VI) is widely used in various industries, however its carcinogenic character makes of the utmost necessity its recovery from the corresponding liquid effluents before their discharge to natural waters. Different separation technologies have found application to remove and/or recover Cr(VI) from these processes wastes [1], among them, adsorption technology can be competitive when the metal is present at low concentrations in the aqueous solution. The importance of this technology on the recovery of this harmful metal is demonstrated by the number of very recent publications in this field, including in these adsorbents are: activated carbon [2–6], nanocomposites [7–14], bio-nanocomposites [15–17], and bioadsorbents [18–22].

One special type of these adsorbents, carbon nanotubes, also is being used in the removal of Cr(VI) from aqueous solutions, summarizing Table 1 some of the most recent advances in the application of these nanotubes in this field of interest.

Being Cyanex 923 an extractant reagent of wide use, the present investigation deals with the adsorption of Cr(VI) using C923-impregnated multi-walled carbon nanotubes. Several variables, which could affect the adsorption process: stirring speed applied on the adsorption system, chromium and HCl concentrations in the aqueous phase, adsorbent dosage, temperature, etc., are investigated. Several equilibrium, kinetics and thermodynamics parameters are also reported. The desorption of Cr(VI)-loaded carbon nanotubes is accomplished using hydrazine sulphate solutions.

2. Experimental set-up

The multi-walled carbon nanotubes used in the investigation was supplied by Fluka (Switzerland) and were used

* Corresponding author.

without further purification, the main characteristics of the adsorbent are given in Table 2.

Cyanex 923 (Solvay, Belgium) is a liquid–liquid extractant composed by four alkyl-phoshine oxides [27], being the active group represented as P=O and with a general structure as R_3PO (R being the alkyl chains), the average molecular weight is 346 and density (20°C) 0.88 g/cm^3, it was also used without further purification. Solvesso 100 (Exxon Chem Iberia, Spain), also used without further purification, is an aromatic diluent widely used in liquid–liquid extraction practice. Cyanex 923 was dissolved in this diluent mainly to decrease the viscosity of the extractant, and to adequate the extractant concentration to its practical use in this work.

Stock Cr(VI) solutions were prepared by dissolving $K_2Cr_2O_7$ (Merck, Germany) in distilled water. All other chemicals were of AR grade.

Impregnation of the multi-walled carbon nanotubes was done by immersion of the pristine nanotubes in a 50% v/v Cyanex 923 in Solvesso 100 solution during 24 h. Then, the mixture was filtered, and the nanotubes were washed twice with distilled water and then dry in a laboratory oven at 50°C until constant weight. Infrared measurements on the C923-impreganted-NTs showed bands at about 1,160 cm^{-1} attributable to the P=O stretching vibration of the phosphine oxide, and weak bands at around 1,300 and 800 cm^{-1} attributable to the δ symmetric mode of the P–CH_3 and to the stretching vibration of the P–C bond, respectively, of the organic extractant. Also, a couple of bands at about 2,900 and 2,850 cm^{-1} can be attributed to the C–H stretching vibrations of the alkyl chains associated to the phosphine oxide group, one peak at about 1,464 cm^{-1} was attributable to the δ asymmetric CH_3 vibration, and bands at 1,410 and near 1,400 cm^{-1} corresponded to the δ symmetric mode of this CH_3 group. The assignation of these bands closely corresponded to data given in the literature [28–30]. These almost unaltered bands with respect to that showed by liquid Cyanex 923, indicated that there was little interaction between the organic extractant and the nanotubes, and thus, the phosphine oxide solution just filled the pores of the carbon material, similarly to the phenomena occurring in the supported liquid membranes technology, in which the extractant filled the micropores of the solid support [31].

Metal adsorption (and desorption) studies were carried out in a glass reactor provided or mechanical shaking *via* a flour blades glass impeller. Metal adsorption (or desorption) was determined by monitoring concentration by AAS (using chromium standards in the 1×10^{-3} to g/L concentrations range) in the aqueous solution as a function of time. Concerning reproducibility data, at a first instance a series of experiments were performed to check the feasibility and consistency of results derived from the same experimental conditions. Reproducibility was good enough for results derived for a fixed period of time using five sets of data.

The metal concentration in the adsorbent was calculated by mass balance. IR measurements were carried out in a Nicolet Magna 550 spectrometer (Japan).

Table 1
Recent literature on the use of multi-walled carbon nanotubes to remove Cr(VI) from solutions

Multi-walled carbon nanotubes and composite	Comments	References
Azadirachta indica	No desorption data	[23]
Anacardium occidentale		[24]
Palladium nanoparticles	Reduction of Cr(VI) to Cr(III)	[25]
Pentaclethra macrophylla		[26]

Table 2
Characteristics of the multi-walled carbon nanotubes

Type	Multi-walled
Melting range	3,652°C–3,697°C
Density	2.1 g/mL
Appearance	Black dust
Purity	≥98% carbon basis
Dimensions	10 ± 1 nm external diameter 4.5 ± 0.5 nm internal diameter 3–6 μm (length)
Maximum adsorption	1,295 cm^3/g
Brunauer–Emmett–Teller	263 m^2/g
Isoelectronic point	1.22

3. Results and discussion

3.1. Chromium(VI) adsorption from pristine and Cyanex 923-impregnated multi-walled carbon nanotubes

In order to investigate the effectiveness of the nanotubes impregnation by Cyanex 923, a series of experiments were conducted using aqueous phases of 0.01 g/L Cr(VI) in 0.1 M HCl medium and adsorbent dosages of 1 g/L. The results of these tests are shown in Fig. 1, and indicated how the impregnation of the carbon nanotubes influenced Cr(VI) adsorption onto both adsorbents. Thus, the use of this alkyl-phosphine oxide to impregnate the carbon nanotubes greatly improved the efficiency of the adsorbent in comparison with the results derived when pristine carbon nanotubes were used in the removal of this harmful metal from aqueous solutions.

3.2. Influence of the stirring speed on chromium(VI) uptake on the impregnated nanotubes

The variation of the stirring speed applied on an adsorption system can have a determinant influence on the quantitative adsorption results, this is because applying the adequate stirring speed, the thickness of the aqueous boundary layer reached a minimum and the adsorption maximizes. In this work, the influence of this variable on Cr(VI) adsorption by the C923-impregnated multi-walled carbon nanotubes had been investigated using an adsorbent dosage of 1 g/L and an aqueous solution of 0.01 g/L in 0.1 M HCl medium. Results from these set of experiments are summarized in Table 3.

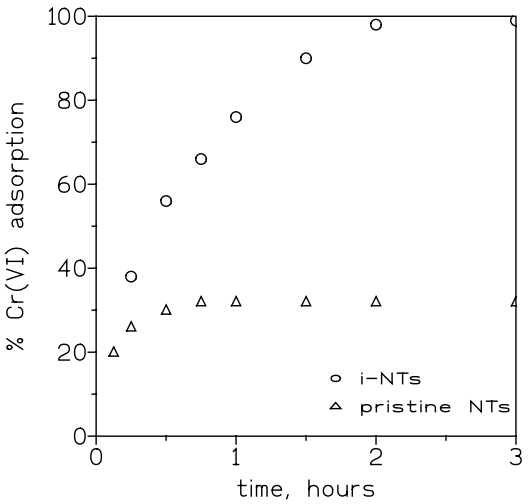

Fig. 1. Chromium(VI) adsorption using pristine multi-walled carbon nanotubes (pristine NTs) and C923-impregnated multi-walled carbon nanotubes (i-NTs). Aqueous phase: 0.01 g/L Cr(VI) in 0.1 M HCl; adsorbent dosage: 1 g/L; temperature: 20°C; stirring speed: 1,000 min^{-1}.

Table 3
Influence of stirring speed on Cr(VI) uptake

Stirring speed, min^{-1}	$[Cr]_{i\text{-}NT}$, mg/g
250	7.6
500	8.0
1,000	9.9
1,500	8.6

Temperature: 20°C; results after 3 h: equilibrium conditions.

It can be seen that Cr(VI) uptake onto the adsorbent increased with the increase of the stirring speed up to 1,000 min^{-1}, and then decreased again. These results can be explained due to the progressive decrease in the thickness of the aqueous boundary layer from 250 to 1,000 min^{-1}, and the aqueous resistance to mass transfer were minimized resulting to that the diffusion contribution of the aqueous species to the adsorption process is assumed to be constant. The decrease of chromium loading onto the adsorbent at the highest stirring speed (1,500 min^{-1}), can be attributable to the formation of local equilibria between the adsorbent particles and the surrounding solution due to this high speed applied on the system. Further adsorption experiments were carried out at 1,000 min^{-1}.

The rate law governing the adsorption process had been modelled using the next models and their corresponding equations:

- diffusion layer-controlled process:

$$\ln\left(1-F\right) = -kt \tag{1}$$

- intraparticle diffusion-controlled process:

$$\ln\left(1-F^2\right) = -kt \tag{2}$$

- moving boundary model:

$$3-3\left(1-F\right)^{2/3} - 2F = kt \tag{3}$$

where F is the fractional approach to equilibrium, defined as:

$$F = \frac{\left[\mathrm{Cr}\right]_{i-\mathrm{NT},t}}{\left[\mathrm{Cr}\right]_{i-\mathrm{NT},e}} \tag{4}$$

being $[Cr]_{i\text{-}NT,t}$ and $[Cr]_{i\text{-}NT,e}$ were Cr(VI) concentrations in the impregnated carbon nantotubes at al elapsed time and at the equilibrium, respectively, and k was the corresponding rate constant. The experimental data at 1,000 min^{-1} were fitted to the three models, and from these fits, it was shown that the rate law governing Cr(VI) uptake onto C923-impreganted multi-walled carbon nanotubes was the moving boundary model (r^2 = 0.9493) and k 0.066 min^{-1}.

3.3. Influence of the temperature on chromium(VI) adsorption on the impregnated nanotubes

The influence of the variation (20°C–60°C) of the temperature on Cr(VI) uptake onto the adsorbent was investigated using aqueous solutions of 0.02 g/L Cr(VI) in 0.1 M HCl medium and adsorbent dosages of 1 g/L. The results from these experiments showed that there was a slight increment of the chromium uptake onto the adsorbent with the increase of the temperature from 20°C (18.8 mg/g) to 60°C (19.6 mg/g).

At a first approximation, there was a relationship between the Cr(VI) distribution coefficient (D_{Cr}) and the temperature accordingly to the expression:

$$\log D_{\mathrm{Cr}} = \frac{\Delta S^\circ}{2.3R} - \frac{\Delta H^\circ}{2.3R}\frac{1}{T} \tag{5}$$

being $\Delta S°$ and $\Delta H°$ the variation of the enthropy and enthalpy in the system as a consequence of Cr(VI) loading onto the adsorbent. D_{Cr} was defined as:

$$D_{\mathrm{Cr}} = \frac{\left[\mathrm{Cr}\right]_{i-\mathrm{NT},e}}{\left[\mathrm{Cr}\right]_{\mathrm{aq},e}} \tag{6}$$

where $[Cr]_{aq,e}$ represented to the chromium concentration in the solution at the equilibrium, and $[Cr]_{i\text{-}NT,e}$ had the same significance than in Eq. (4). Thus, a plot of $\log D_{Cr}$ vs. $1/T$ allowed estimated the thermodynamic character ($\Delta H°$) of the chromium uptake process and the variation in randomness ($\Delta S°$) of such uptake. This plot (r^2 = 0.9699) resulted in that Cr(VI) adsorption onto the C923-impreganted carbon nanotubes had an endothermic character with an increment of the process randomness.

Also,

$$\Delta G^\circ = \Delta H^\circ - T\Delta S^\circ \tag{7}$$

and at 20°C, the adsorption process was spontaneous. Table 4 shows the estimated values of $\Delta H°$, $\Delta S°$ and $\Delta G°$ for this system.

3.4. Influence of the variation of the acidity of the aqueous phase on chromium(VI) adsorption

The variation of the HCl concentration of the aqueous solution on Cr(VI) uptake onto the impregnated carbon nanotubes was investigated using aqueous solutions of 0.01 g/L Cr(VI) in different HCl concentrations (0.1–2 M), and adsorbent dosages of 1 g/L. The results from the experiments are summarized in Table 5, which shows that the increase in the HCl concentration from 0.1 to 2 M resulted in a decrease of the chromium concentration loaded onto the impregnated adsorbent. These results can be attributable to:

- that Cyanex 923 extracted HCl from aqueous solutions [29], and this extraction (adsorption) competed with that of Cr(VI), resulting in the decrease of the adsorption of this latter solute, and:
- it is also described in the literature [32], the existence of CrO_3Cl^- species in HCl solutions, thus, this decrease in metal adsorption can be due to the less extractability (adsorbability) of this chromium species by Cyanex 923.

3.5. Influence of the initial metal concentration on chromium(VI) uptake onto the nanotubes

The variation of the chromium concentration (0.01–0.2 g/L) in the aqueous solution on the metal adsorption onto the adsorbent was also investigated. In this case, the adsorbent dosage was of 1 g/L, whereas the aqueous solutions contained different metal concentrations in 0.1 M HCl medium. The results from these experiments are shown in Fig. 2, plotting metal concentrations in the adsorbent vs. the initial chromium concentration in the aqueous solution.

The results showed that the increase of the initial Cr(VI) concentration in the aqueous phase resulted in a decrease of the percentage of the metal adsorption onto the adsorbent, though in all the cases, the equilibrium was reached within 3 h of contact between the solution and the adsorbent. It is worth to note here that. al low Cr(VI) concentrations (<0.1 g/L) in the solution, $HCrO_4^-$ is the unique and predominant metal species present at acidic-neutral pH values, but from 0.1 g/L Cr(VI) concentration in the solution, the fraction of $Cr_2O_7^{2-}$ species in the aqueous phase was noticed, increasing this fraction with the increase of Cr(VI) concentration in the solution, until a point in which $Cr_2O_7^{2-}$ species become predominant over $HCrO_4^-$ species.

The adsorption results were used to model the adsorption isotherm related to the present system. Both the Langmuir and Freundlich isotherms had been used to model the experimental data, being both widely used in the modelling of adsorption or ion exchange processes [33].

The Langmuir models are valid for monolayer adsorption onto a surface containing a limited number of identical sites. The Langmuir-Type 1 [Eq. (8)] and Langmuir-Type 2 [Eq. (9)] in their linear forms describing these models are:

$$\frac{[\mathrm{Cr}]_{\mathrm{aq},e}}{[\mathrm{Cr}]_{i-\mathrm{NT},e}} = \frac{1}{K_L[\mathrm{Cr}]_{i-\mathrm{NT},m}} + \frac{1}{[\mathrm{Cr}]_{i-\mathrm{NT},e}}[\mathrm{Cr}]_{\mathrm{aq},e} \quad (8)$$

$$\frac{1}{[\mathrm{Cr}]_{c,e}} = \frac{1}{[\mathrm{Cr}]_{c,m}} + \frac{1}{b[\mathrm{Cr}]_{c,m}}\frac{1}{[\mathrm{Cr}]_{s,e}} \quad (9)$$

where K_L is a constant related to the model, $[Cr]_{i\text{-}NT,m}$ is the maximum metal uptake in the carbon nanotubes, and $[Cr]_{aq,e}$ is the equilibrium chromium(VI) concentration in the solution.

The Freundlich model, is an empirical expression describing adsorption processes onto heterogeneous surfaces, having the adsorbent surface sites with a variation of binding energies. In this case, the equation also in its linear form is:

$$\ln[\mathrm{Cr}]_{i-\mathrm{NT},e} = \ln K_F + \frac{1}{n}\ln[\mathrm{Cr}]_{\mathrm{aq},e} \quad (10)$$

where K_F and n are parameters related to the Freundlich model. The results from these fits indicated that the

Table 4
Estimated thermodynamic values for Cr(VI) adsorption

$\Delta H°$, kJ/mol	–23
$\Delta S°$, J/mol·K	101
$\Delta G°$, kJ/mol	–6

Table 5
Chromium(VI) uptake at various HCl concentrations

HCl, M	$[Cr]_{i\text{-}NT,e}$
0.1	9.9
1	9.2
2	8.0

Temperature: 20°C; time: 3 h; stirring speed: 1,000 min^{-1}.

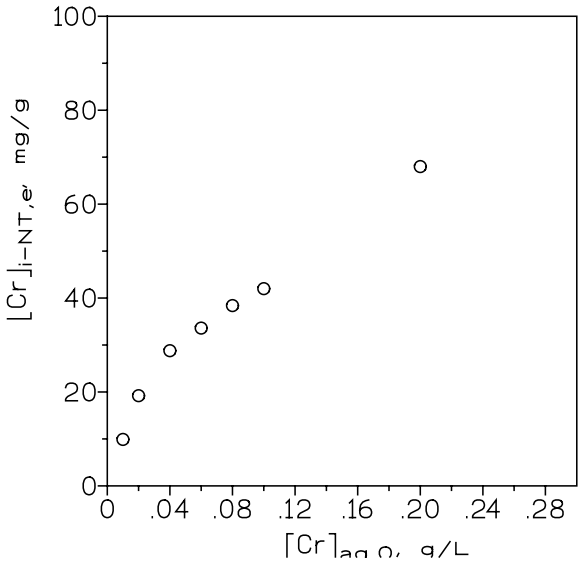

Fig. 2. Variation of the chromium concentration in the adsorbent at various initial metal concentrations in the aqueous solution. Aqueous phase: chromium(VI) in 0.1 M HCl; temperature: 20°C; time: 3 h (equilibrium conditions); stirring speed: 1,000 min^{-1}.

experimental data best responded (r^2 = 0.9218) to the Freundlich isotherm, being lnK_F 2.84 and n equal to 4, thus, the adsorption process is favourable since $1 < n < 10$ [34].

3.6. Influence of the adsorbent dosage on chromium(VI) adsorption

It was investigated the influence of the adsorbent dosage (0.5–1 g/L) on Cr(VI) removal from the solution using aqueous phases of 0.1 g/L Cr(VI) in 0.1 M HCl. The results of the investigation are shown in Fig. 3 plotting $[Cr]_{aq,t}/[Cr]_{aq,0}$ vs. time; these results indicated that chromium was almost quantitatively removed (about 99%) from the solution using these two adsorbent dosages, but the time to achieve this goal was greatly dependent on the adsorbent dosage used in the experimentation.

Using an adsorbent dosage of 1 g/L, the equilibrium was reached within 2 h (9.9 mg/g chromium loading onto the adsorbent), whereas if the adsorbent dosage was of 0.5 g/L, the time necessary to reach equilibrium conditions increased up to 5 h (19.6 mg/g chromium loading onto the impregnated adsorbent). The adsorption results were used to model the kinetics equation [35] describing the adsorption process using these two adsorbent dosages:

- pseudo-first-order model, this model can be expressed accordingly with the next equation:

$$\ln\left(\left[\mathrm{Cr}\right]_{i-\mathrm{NT},e}-\left[\mathrm{Cr}\right]_{i-\mathrm{NT},t}\right)=\ln\left[\mathrm{Cr}\right]_{i-\mathrm{NT},e}-K_{\mathrm{ps1}}t \tag{11}$$

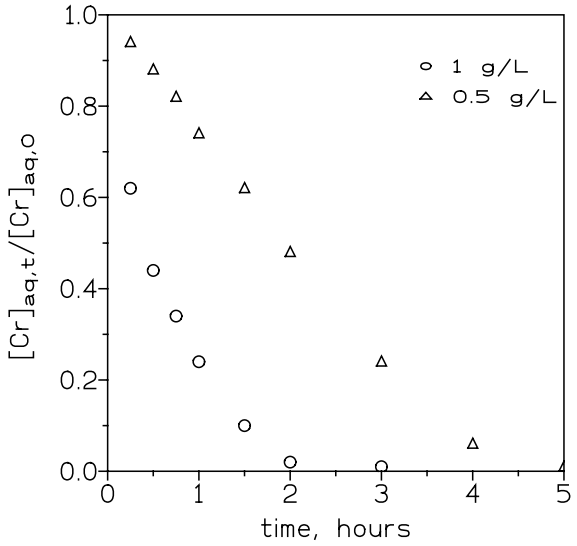

Fig. 3. Variation of $[Cr]_{aq,t}/[Cr]_{aq,0}$ relationship vs. time at two adsorbent dosages. Temperature: 20°C; stirring speed: 1,000 min^{-1}.

where $[Cr]_{i\text{-}NT,e}$ and $[Cr]_{i\text{-}NT,e}$ are the chromium concentrations in the nanotubes at equilibrium at an elapsed time, respectively, t is the time and K_{ps1} is the constant related to this model,

- pseudo-second-order model, in this model, the equation used is:

$$\frac{t}{\left[\mathrm{Cr}\right]_{i-\mathrm{NT},t}}=\frac{1}{K_{\mathrm{ps2}}\left[\mathrm{Cr}\right]^2_{i-\mathrm{NT},e}}+\frac{1}{\left[\mathrm{Cr}\right]_{i-\mathrm{NT},e}}t \tag{12}$$

in this case, K_{ps2} is the constant related to this model.

From these fit, it was concluded that in the case of the adsorbent dosage of 1 g/L, the adsorption process responded (r^2 = 0.9955) to the pseudo-second-order kinetic model [Eq. (12)], thus, the adsorption was attributable to a chemisorption process, however in the case of the lower adsorbent dosage of 0.5 g/L, chromium uptake onto the impregnated adsorbent best fitted (r^2 = 0.9259) to the first-order kinetic equation:

$$\ln\left[\mathrm{Cr}\right]_{\mathrm{aq},t}=\ln\left[\mathrm{Cr}\right]_{\mathrm{aq},0}-K_1t \tag{13}$$

where K_1 is the constant associated to the model. Table 6 summarized the values of the parameters of Eqs. (12) and (13).

The values of $[Cr]_{aq,0}$ (0.01 g/L) and $[Cr]_{i\text{-}NT,e}$ (13 mg/g) compared relatively well with the respective values of 0.01 g/L and 9.9 mg/g experimentally found.

3.7. Influence of the aqueous ionic strength on chromium(VI) uptake onto the nanotubes

Results derived from subsection 3.4. (Table 5) showed that when HCl is the main source for the ionic strength (I_M, ionic strength in the molar scale) in the solution, and increase of this variable from 0.1 M HCl (I_M = 0.1) to 2 M HCl (I_M = 2) produced a decrease in the metal loading onto the adsorbent. Further investigations about the influence of this variable on chromium uptake had been carried out by varying the source of the ionic strength by the use of different salts ($LiNO_3$, LiCl, $NaClO_4$, Li_2SO_4 and NaF). In these series of experiments, the adsorbent dosage was of 1 g/L, whereas the aqueous solutions contained 0.01 g/L Cr(VI) in solutions of I_M = 0.1. The results from this experimentation are shown in Table 7.

These results demonstrated the importance of the presence of the acid in the aqueous solution to yield a reasonable chromium loading onto the adsorbent. This importance was attributable to the type of the adsorption process which took into consideration the form in which Cyanex 923-extracted Cr(VI) from acidic media [36]:

Table 6
Kinetic parameters associated to the adsorption of Cr(VI) using different adsorbent dosages

Adsorbent dosage, g/L	Model	K_1, min^{-1}	$[Cr]_{aq,0}$, g/L	K_{ps2}, g/min·mg	$[Cr]_{i\text{-}NT,e}$, mg/g
0.5	Pseudo-first-order	0.032	0.01		
1	Pseudo-second-order			1.9×10^{-3}	13

Table 7
Variation in chromium uptake with the source of the ionic strength

HCl	9.9 mg/g
$LiNO_3$	0.8 mg/g
LiCl	0.4 mg/g
$NaClO_4$	2.0 mg/g
Li_2SO_4	1.6 mg/g
NaF	0.6 mg/g

Temperature: 20°C; time: 3 h (equilibrium conditions); stirring speed: 1,000 min^{-1}.

$$2C923-NT+H^+_{aq}+HCrO^-_{4_{aq}} \Leftrightarrow H_2CrO_4\cdot 2C923-NT \quad (14)$$

thus, the presence of protons in the aqueous solution shifted the above equilibrium to the right, increasing metal loading onto the C923-impregnated multi-walled carbon nanotubes. The removal of chromium(VI) from the solution involved the solvation of chromium(VI) species by the phosphine oxide *via* the donation on electron–pair from the extractant (P=O:). The phosphine oxide competed favourably with water molecules, replacing them in the primary coordination sphere of chromium(VI) species.

3.8. Chromium(VI) desorption

In the present investigation, the desorption of Cr(VI) from the metal-loaded nanotubes was studied using hydrazine sulphate solutions, at the same time, in the desorption process, Cr(VI) is reduced to the less hazardous Cr(III) oxidation state, accordingly to [37]:

$$4HCrO^-_4+10H^++3N_2H_4\cdot H_2SO_4 \rightarrow 4Cr^{3+}+16H_2O+3N_2+3SO^{2-}_4 \quad (15)$$

Desorption experiments were carried out with aqueous solutions containing 25–50 g/L of hydrazine sulphate and 2 mg/g Cr(VI)-loaded C923-impregnated carbon nanotubes, at a 25 mL/g solution volume/weighed carbon nanotubes relationship, and 20°C. The results from these experiments can be summarized as:

- the equilibrium is reached within 5 min of reaction,
- the variation in the hydrazine sulphate solution concentration has little effect on the reaction yield (97% chromium recovery from loaded nanotubes),
- the desorbed solution contained a Cr(III) concentration near 8 times the initial Cr(VI) concentration in the feed solution (0.01 g/L) of the adsorption experiments.

4. Conclusions

Impregnation of multi-walled carbon nanotubes by the phosphine oxide Cyanex 923 increased the performance of these nanotubes towards Cr(VI) removal from aqueous solutions. The adsorption of Cr(VI) onto C923-impregnated multi-walled carbon nanotubes is dependent on the HCl concentration of the aqueous solution, decreasing this adsorption when the acid concentration increased from 0.1 to 2 M. At the optimum stirring speed, the rate law governing The adsorption is exothermic ($\Delta H°$ = –15 kJ/mol), and non-spontaneous (positive $\Delta G°$ valour), and the metal adsorption responded to the Freundlich isotherm. Cr(VI) can be desorbed from metal-loaded carbon nanotubes by the use of hydrazine sulphate solutions, which releases chromium to the aqueous solution as the less hazardous (III) valence state.

Acknowledgement

To the CSIC (Spain) for Project 202250E019.

References

[1] N. Itankar, Y. Patil, Assessing physicochemical technologies for removing hexavalent chromium from contaminated waters—an overview and future research directions, Water Air Soil Pollut., 233 (2022) 355, doi: 10.1007/s11270-022-05745-z.
[2] M.A. Hamdan, E.T. Sublaban, J.J. Al-Asfar, M.A. Banisaid, Wastewater treatment using activated carbon produced from oil shale, J. Ecol. Eng., 24 (2023) 131–139.
[3] I. Loulidi, M. Jabri, A. Amar, A. Kali, A. Alrashdi, C. Hadey, M. Ouchabi, P.S. Abdullah, H. Lgaz, Y. Cho, F. Boukhlifi, Comparative study on adsorption of crystal violet and chromium(VI) by activated carbon derived from spent coffee grounds, Appl. Sci., 13 (2023) 985, doi: 10.3390/app13020985.
[4] J. Sharma, M. Sharma, S. Nigam, M. Joshi, Environmental-friendly algal-mediated magnetic activated carbon for adsorptive removal of contaminants from water, Chem. Phys. Impact, 6 (2023) 100169, doi: 10.1016/j.chphi.2023.100169.
[5] L. Qiu, Y. Wang, R. Sui, C. Zhu, Y. Weiwei, Y. Yu, J. Li, Preparation of a novel metal-free polypyrrole-red phosphorus adsorbent for efficient removal of Cr(VI) from aqueous solution, Environ. Res., 224 (2023) 115458, doi: 10.1016/j.envres.2023.115458.
[6] H. Zuo, Y. Xia, H. Liu, Z. Liu, Y. Huang, Preparation of activated carbon with high nitrogen content from agro-industrial waste for efficient treatment of chromium(VI) in water, Ind. Crops Prod., 194 (2023) 116403, doi: 10.1016/j.indcrop.2023.116403.
[7] N. Shabelskaya, M. Egorova, A. Radjabov, M. Burachevskaya, I. Lobzenko, I.T. Minkina, S. Sushkova, Formation of biochar nanocomposite materials based on $CoFe_2O_4$ for purification of aqueous solutions from chromium compounds(VI), Water, 15 (2023) 93, doi: 10.3390/w15010093.
[8] N. Redwan, D. Tsegaye, B. Abebe, Synthesis of iron-magnetite nanocomposites for hexavalent chromium sorption, Res. Chem., 5 (2023) 100797, doi: 10.1016/j.rechem.2023.100797.
[9] P. Semalti, J. Saroha, J.S. Tawale, S.N. Sharma, Visible-light driven noble metal (Au, Ag) permeated multicomponent Cu_2ZnSnS_4 nanocrystals: a potential low-cost photocatalyst for textile effluents and heavy metal removal, Environ. Res., 217 (2023) 114875, doi: 10.1016/j.envres.2022.114875.
[10] F. Liu, S. Wang, B. Hu, Electrostatic self-assembly of nanoscale FeS onto MXenes with enhanced reductive immobilization capability for U(VI) and Cr(VI), Chem. Eng. J., 456 (2023) 141100, doi: 10.1016/j.cej.2022.141100.
[11] A. Bukhari, I. Ijaz, H. Zain, U. Mehmood, M. Mudassir Iqbal, E. Gilani, A. Nazir, Introduction of CdO nanoparticles into graphene and graphene oxide nanosheets for increasing adsorption capacity of Cr from wastewater collected from petroleum refinery, Arabian J. Chem., 16 (2023) 104445, doi: 10.1016/j.arabjc.2022.104445.
[12] M. Arif, Extraction of iron(III) ions by core-shell microgel for in situ formation of iron nanoparticles to reduce harmful pollutants from water, J. Environ. Chem. Eng., 11 (2023) 109270, doi: 10.1016/j.jece.2023.109270.
[13] F. Liu, Y. Lou, F. Xia, B. Hu, B. Immobilizing nZVI particles on MBenes to enhance the removal of U(VI) and Cr(VI)

by adsorption-reduction synergistic effect, Chem. Eng. J., 454 (2023) 140318, doi: 10.1016/j.cej.2022.140318.
[14] Z. Sheerazi, S.A., Khan, S.A. Chaudhry, T.A. Khan, Non-linear modelling of adsorption isotherm and kinetics of chromium(VI) and celestine blue attenuation using a novel poly(curcumin-citric acid)/$MnFe_2O_4$ nanocomposite, Model. Earth Syst. Environ., 9 (2023) 881–899.
[15] X. Liu, Y. Zhang, Y. Liu, T. Zhang, Magnetic red mud/chitosan based bionanocomposites for adsorption of Cr(VI) from aqueous solutions: synthesis, characterization and adsorption kinetics, Polym. Bull., 80 (2023) 2099–2118.
[16] T.S. Ngo, C.T. Tracey, A.G. Navrotskaya, A.V. Bukhtiyarov, P.V. Krivoshapkin, E.F. Krivoshapkina, Reusable carbon dot/chitin nanocrystal hybrid sorbent for the selective detection and removal of Cr(VI) and Co(II) ions from wastewater, Carbohydr. Polym., 304 (2023) 120471, doi: 10.1016/j.carbpol.2022.120471.
[18] A. Kalsoom, R. Batool, N. Jamil, Bacterial journey of micro- and nano-adsorption mechanisms for chromate elimination: a prospective study, Res. J. Chem. Environ., 26 (2022) 131–142.
[19] U.F.C. Sayago, V. Ballesteros Ballesteros, Development of a treatment for water contaminated with Cr(VI) using cellulose xanthogenate from *E. crassipes* on a pilot scale, Sci. Rep., 13 (2023) 1970, doi: 10.1038/s41598-023-28292-x.
[20] S.S. Varnamkhasti, M.R. Samani, D. Toghraie, D. Removal of chromium(VI) from aqueous environments using composites of polyaniline-cherry leaves, J. Environ. Manage., 332 (2023) 117359, doi: 10.1016/j.jenvman.2023.117359.
[21] X. Zhang, K. Ma, H. Peng, Y. Gong, Y. Huang, Imidazolium functionalized polysulfone/DTPA-chitosan composite beads for simultaneous removal of Cr(VI) and Cu(II) from aqueous solutions, Sep. Purif. Technol., 310 (2023) 123145, doi: 10.1016/j.seppur.2023.123145.
[22] M.R. Shahab, H.M. Yaseen, Q. Manzoor, A. Saleem, A. Sajid, Q.M. Malik, S. Ahmed, Adsorption of methyl orange and chromium(VI) using *Momordica charantia* L. leaves: a dual functional material for environmental remediation, J. Iran. Chem. Soc., 20 (2023) 577–590.
[23] H. Uthayakumar, P. Radhakrishnan, K. Shanmugam, O.S. Kushwaha, Growth of MWCNTs from *Azadirachta indica* oil for optimization of chromium(VI) removal efficiency using machine learning approach, Environ. Sci. Pollut. Res., 29 (2022) 34841–34860.
[24] J.F. Amaku, S.A. Ogundare, K.G. Akpomie, C.M. Ngwu, J. Conradie, Enhanced chromium(VI) removal by *Anacardium occidentale* stem bark extract-coated multi-walled carbon nanotubes, Int. J. Environ. Sci. Technol., 19 (2022) 4421–4434.
[25] I. Gözeten, M. Tunç, Palladium nanoparticles supported on multi-walled carbon nanotube (MWCNT) for the catalytic hexavalent chromium reduction, Mater. Chem. Phys., 278 (2022) 125628, doi: 10.1016/j.matchemphys.2021.125628.
[26] J.F. Amaku, S.A. Ogundare, K.G. Akpomie, J. Conradie, *Pentaclethra macrophylla* stem bark extract anchored on functionalized MWCNT-spent molecular sieve nanocomposite for the biosorption of hexavalent chromium, Int. J. Phytorem., 24 (2022) 301–310.
[27] E. Dziwinski, J. Szymanowski, Composition of CYANEX 923, CYANEX 925, CYANEX 921 and TOPO, Solvent Extr. Ion Exch., 16 (1998) 1515–1525.
[28] F.J. Alguacil, F.A. Lopez, The extraction of mineral acids by the phosphine oxide Cyanex 923, Hydrometallurgy, 42 (1996) 245–255.
[29] J. Lu, Z. Wei, D. Li, G. Ma, Z. Jiang, Recovery of Ce(IV) and Th(IV) from rare earths(III) with Cyanex 923, Hydrometallurgy, 50 (1998) 77–87.
[30] W. Liao, G. Yu, D. Li, Solvent extraction of cerium(IV) and fluorine(I) from sulphuric acid leaching of bastnasite by Cyanex 923, Solvent Extr. Ion Exch., 19 (2001) 243–259.
[31] F.J. Alguacil, M. Alonso, F. Lopez, A. Lopez-Delgado, Uphill permeation of Cr(VI) using Hostarex A327 as ionophore by membrane-solvent extraction processing, Chemosphere, 72 (2008) 684–689.
[32] A. Agrawal, C. Pal, K.K. Sahu, Extractive removal of chromium(VI) from industrial waste solution, J. Hazard. Mater., 159 (2008) 458–464.
[33] A. Ahmad, A. Khatoon, S.-H. Mohd-Setapar, R. Kumar, M. Rafatullah, Chemically oxidized pineapple fruit peel for the biosorption of heavy metals from aqueous solutions, Desal. Water Treat., 57 (2016) 6432–6442.
[34] S. Zhou, W. Li, W. Liu, J. Zhai, Removal of metal ions from cyanide gold extraction wastewater by alkaline ion-exchange fibers, Hydrometallurgy, 215 (2023) 105992, doi: 10.1016/j.hydromet.2022.105992.
[35] A. Yar, Ş. Parlayici, Carbon nanotubes/polyacrylonitrile composite nanofiber mats for highly efficient dye adsorption, Colloids Surf., A, 651 (2022) 129703, doi: 10.1016/j.colsurfa.2022.129703.
[36] F.J. Alguacil, J.I. Robla, Transport of chromium(VI) across a supported liquid membrane containing Cyanex 921 or Cyanex 923 dissolved in Solvesso 100 as carrier phase: estimation of diffusional parameters, Membranes, 13 (2023) 177, doi: 10.3390/membranes13020177.
[37] F.J. Alguacil, M. Alonso, Chromium(VI) removal through facilitated transport using CYANEX 923 as carrier and reducing stripping with hydrazine sulfate, Environ. Sci. Technol., 37 (2003) 1043–1047.